

Hydrogen-induced structural changes in tetrahedral amorphous carbon

G. Kopidakis,* C. Z. Wang, C. M. Soukoulis, and K. M. Ho

Ames Laboratory and Department of Physics and Astronomy, Iowa State University, Ames, Iowa 50011

(Received 10 June 1998)

The influence of hydrogen on the structure and properties of tetrahedral amorphous carbon (ta-C) is studied by tight-binding molecular-dynamics simulations. The results show that hydrogen tends to break carbon-carbon bonds in ta-C. Reduction of C-C coordinations makes ta-C softer and introduces more electronic states in the energy-gap region. [S0163-1829(98)00945-X]

Tetrahedral amorphous carbon (ta-C) films have attracted considerable attention in recent years.¹ The unique properties of this material, such as mechanical hardness, optical transparency, and chemical inertness make it potentially useful for technological applications as protective coating. In the past several years, many efforts have been made to elucidate the microscopic structure and physical properties of this disordered form of carbon.²⁻⁹ An outstanding issue is to understand the influence of hydrogen on the structure and properties of ta-C,⁶ since many tetrahedral a-C samples contain a certain amount of hydrogen atoms. Although there has been a number of computer simulation studies of hydrogenated amorphous carbon (a-C:H) at a density regime lower than that of typical ta-C samples,^{7,10-12} with all the recent developments in preparation and characterization of ta-C films, it is now highly desirable to investigate the effects of hydrogen in high-density ta-C networks.

In this paper, we present a tight-binding molecular-dynamics (TBMD) simulation study of hydrogen in ta-C. Starting with a pure ta-C sample generated previously,¹³ we add different amounts of atomic hydrogen and examine the changes in the structural, electronic, and mechanical properties of the ta-C network as the hydrogen concentration varies. Our study provides a microscopic picture illustrating how hydrogen affects the structure and properties of ta-C.

Details of the TBMD scheme have been described in Ref. 14. In the present study, we use the tight-binding potential of Xu *et al.*¹⁵ to describe the interaction between the carbon atoms. The interaction between the carbon and hydrogen atoms was then determined by fitting to the electronic structure, binding energy, and vibrational frequencies of the methane (CH₄) molecule.¹⁶ Specifically, the hopping parameters between the *s* orbital of hydrogen and the *s* and *p* orbitals of carbon $V_{ss\sigma}$ and $V_{sp\sigma}$ as a function of carbon hydrogen interatomic distance were fitted to the local-density approximation (LDA) electronic energy levels of the CH₄ for different interatomic separations r_{CH} and the bending modes of the CH₄ molecule. The on-site energy for hydrogen E_H was adjusted to fit the *ab initio* result of the Mulliken charge population at each atom of CH₄.¹⁷ After obtaining the C-H tight-binding parameters, the repulsive potential between carbon and hydrogen atoms is then fitted to the LDA result of binding energy of CH₄ molecule.¹⁸ In Fig. 1 the carbon-hydrogen tight-binding hopping parameters and the repulsive potential as a function of the interatomic distance r_{CH} are plotted. More details about the C-H tight-binding model can be found in Ref. 16.

The above model for C-H interactions along with the carbon tight-binding potential of Xu *et al.* give very good results for hydrocarbon molecules. The equilibrium distance for CH₄ is at $r_{CH0}=1.104$ Å compared with the experimental $r_{CH0}=1.087$ Å (Ref. 19) and the binding energy is -18.884 eV compared with the experimental -17.019 eV and the local spin-density approximation result of -18.89 eV.²⁰ The symmetric and antisymmetric bending modes for CH₄ are found to be 0.191 and 0.169 eV, respectively, compared with 0.190 and 0.1625 eV of the experiment.²¹ The symmetric and antisymmetric stretching modes are 0.381 and 0.364 eV compared with the experimental 0.374 and 0.362 eV, respectively.²¹ The model also describes well the structures, binding energies, and vibrations of ethylene (C₂H₄), ethane (C₂H₆),¹⁶ and the properties of larger hydrocarbon molecules as well as the energies of interstitial hydrogen in diamond.²² In particular, the bond-centered site is found to be the lowest-energy interstitial site for hydrogen in diamond, in agreement with first-principles calculations²³ and results on muonium in diamond.²⁴

The starting configuration for our tight-binding molecular-dynamics simulation is a tetrahedral amorphous carbon structure generated by quenching liquid carbon down to room temperature, as described in Ref. 13. The cubic cell consisted of 216 carbon atoms, with 158 (73%) fourfold and 58 (27%) threefold. The sides of the box are 10.875 Å. In order to study the effects of hydrogen on the structure and

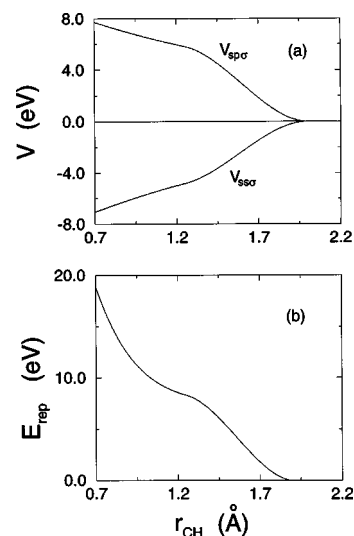


FIG. 1. The C-H parameters used in the TBMD simulation as a function of the interatomic separation.

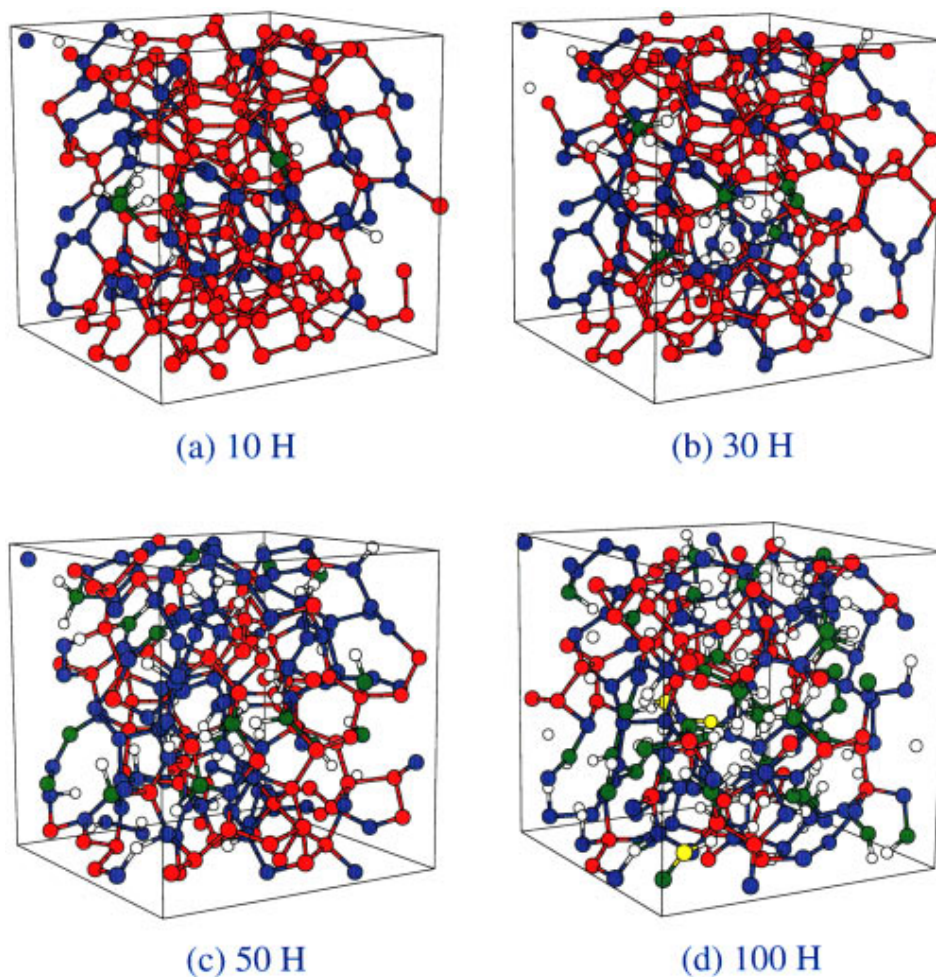


FIG. 2. (Color) ta-C:H structures with 4.4 at. % H (a), 12.2 at. % (b), 18.8 at. % (c), and 31.6 at. % (d). Hydrogen atoms are represented by the small white balls. The red, blue, green, and yellow balls are the carbon atoms with four, three, two, and one C-C bonds, respectively.

properties of ta-C, different numbers of hydrogen atoms are added, i.e., 10, 30, 50, 100 that correspond to atomic-hydrogen concentrations of about 4.4%, 12.2%, 18.8%, 31.6%, respectively. For each hydrogen concentration, the system is annealed by heating up to 2000 K and then cooling down to 0 K. The time step used in the molecular-dynamics simulation was 0.7×10^{-16} s and 1000 molecular-dynamics steps were performed for each temperature from 2000 K down to 0 K with 500 K difference. The volume of the box remained constant during the temperature-controlled quenching process, but it was allowed to relax at zero temperature to the equilibrium volume. The relaxed structures of the resulting a-C:H samples are presented in Fig. 2. The labels (a), (b), (c), and (d) are used for the samples with 10, 30, 50, and 100 hydrogen atoms, respectively. In this figure, the hydrogen atoms are represented by the small white balls. Different colors are used to represent carbon atoms with different numbers of C-C bonds. The red, blue, green, and yellow colors indicate that the carbon atoms have four, three, two, and one carbon-carbon bonds, respectively. It is clearly seen from the figure that hydrogen atoms systematically reduce the carbon-carbon bonds in the ta-C samples. There are 141 red atoms in the sample with 10 hydrogen atoms while only 70 red atoms are retained in the a-C sample with 100 hydrogen atoms. At the same time, the number of green and yellow atoms increase from 5 to 43 as the hydrogen atoms in-

creases from 10 to 100. The carbon coordination number drops significantly, from 3.73 for the pure a-C to 3.11 for the sample with 100 hydrogen atoms. Detail counting of C-C bonds as the function of hydrogen concentration are listed in Table I. It is clear that C-C bonds are broken by the hydrogen atoms. It is interesting to note that the total sp^3 fraction (including the C-H bonds) decreases only from 0.71 to 0.63 when the number of hydrogen atoms increases from 10 to 100, although the fraction of fourfold carbon bonded sites has dropped from 0.65 to 0.32. The total sp^3 fraction is also not a monotonous function of hydrogen concentration, as one can see from Table I. This phenomenon is understandable because the reduction of C-C bonds induced by the hydrogen can be compensated by the new forming C-H bonds. Besides the hydrogen atoms bonded to one carbon atom, the existence of hydrogen at the bond center between carbons (C-H-C bonds) is evident from these pictures. However, the fraction of hydrogen bond-center sites is found to decrease rapidly as the hydrogen content increases. There are 70% of bond-center hydrogen atoms in the 10-hydrogen sample, but only 8% of such atoms in the 100-hydrogen sample. In Table I, some bonding data of hydrogen are also shown as a function of hydrogen concentration.

The total and partial pair-correlation functions calculated from these a-C:H samples are shown in Fig. 3. The peaks A and C in the total pair-correlation function $g(r)$ are mainly

TABLE I. Distribution of carbon and hydrogen atoms in ta-C:H samples. The cutoff distances for the C-C and C-H bonds are 1.93 and 1.30 Å, respectively. The coordinations in this table include both C-C bonds and C-H bonds.

Number of H in the ta-C:H	0	10	30	50	100
number of C atoms with 4 C-C bonds	158	141	124	86	70
number of C atoms with 3 C-C bonds	58	70	84	112	103
number of C atoms with 2 C-C bonds	0	5	8	18	40
number of C atoms with 1 C-C bond	0	0	0	0	3
average C-C bonds	3.73	3.63	3.54	3.31	3.11
number of C atoms with 4 coordinations	158	153	157	136	137
number of C atoms with 3 coordinations	58	63	59	78	72
number of C atoms with 2 coordinations	0	0	0	2	7
number of C atoms with 1 coordination	0	0	0	0	0
average coordinations	3.73	3.71	3.73	3.62	3.60
number of H atoms with 2 C neighbors		7	12	17	8
number of H atoms with 1 C neighbor		3	17	33	90
number of H atoms with 0 C neighbor		0	1	0	2

coming from the first- and second-neighbor distances between carbon and hydrogen atoms, while the peaks *B* and *D* are the first- and second-neighbor distances among the carbon atoms. This can be seen more clearly from the partial pair-correlation functions g_{ch} and g_{cc} as shown in Figs. 3(b) and 3(c), respectively. From the partial C-H pair-correlation functions of Fig. 3(b), it is deduced that the average C-H bond length is 1.134, 1.138, 1.137, and 1.113 Å, respec-

tively, for the ta-C:H samples with 10, 30, 50 and 100 hydrogen atoms. These average bond lengths are slightly longer than the C-H distance in CH₄ molecule. We also note that the C-H bond length of the 100-hydrogen ta-C:H sample is shorter than that in the other three samples. This difference may be attributed to the rapid decrease of the percentage of the bond-center hydrogen atoms in this sample since C-H bonds are in general stronger than C-H-C bonds and thus shorter bond lengths. The peak positions of C-H second neighbors are found to shift toward large distance, with 1.89, 2.01, 2.07, and 2.12 Å, respectively, for the samples of 10, 30, 50, and 100 hydrogen atoms. From the partial C-C pair-correlation functions of Fig. 3(c), the average C-C bond length is calculated to be 1.55 Å for all hydrogen concentrations. The C-C second-neighbor peaks are at 2.49, 2.54, 2.53, and 2.45 Å, is respectively. Figure 3(c) also shows that the partial pair-correlation function g_{cc} is broadened as the hydrogen concentration increases. This suggests that hydrogen atoms induce disorder in the ta-C samples.

In order to see how the presence of hydrogen influences the electronic properties of the ta-C sample, we have performed a local electronic density of states analysis for the carbon and hydrogen atoms, respectively. These results are plotted in Fig. 4 for the four samples with different hydrogen concentrations. We found that the bonding and antibonding states on hydrogen atoms are well separated in all samples. There are one or two states in the middle of the gap in the samples with 30 and 100 hydrogen atoms due to the presence of free (nonbonded) hydrogen atoms in these samples. Otherwise the local density of states of the hydrogen is very similar to that of monohydride on diamond (111) surface.²⁵ It is interesting to note that the increase in hydrogen content seems to increase the number of electronic states of the a-C samples in the gap region (i.e., near the Fermi-energy level). This is in contrast to the case of hydrogen in a-Si where hydrogen reduces the electronic states in the gap region because hydrogen atoms can passivate silicon dangling bonds and hence reduce the defect states in the gap region.²⁶ The increase in carbon electronic density of states in the gap region is consistent with the atomic picture that C-C bonds are broken under the influence of hydrogen. Since the states in

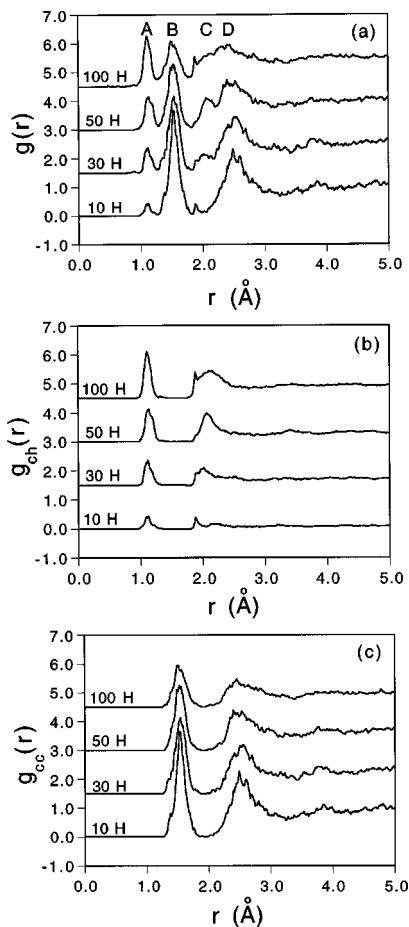


FIG. 3. (a) Total pair-correlation functions; (b) C-H pair-correlation functions; (c) C-C pair-correlation functions.

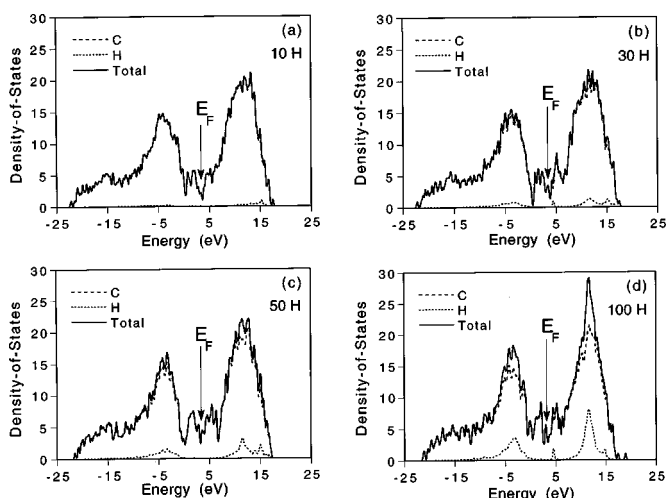


FIG. 4. Electronic density of states of the a-C:H sample.

the gap region are the contributions from the π states of the carbon atoms, decreasing C-C bonds will increase the number of π states and hence the density of states in the gap region.

Another related question is how the presence of hydrogen affects the hardness of the ta-C samples. This problem has been addressed using classical interatomic potentials¹⁰ and experiment.⁶ In this paper, we studied the dependence of the bulk modulus on the hydrogen concentration. The bulk modulus is calculated from the energy vs volume curve through fitting with the universal binding-energy curve.²⁷ The total energies of the samples at different volumes are obtained by relaxing the structures with different cubic cell sizes through TBMD. Figure 5 shows the bulk modulus as a function of the hydrogen concentration. It is clear that it drops with increasing hydrogen content, i.e., the material becomes softer when more hydrogen is present. Hardness decrease with the increase of hydrogen content has also been observed in low-density a-C:H in the molecular-dynamics

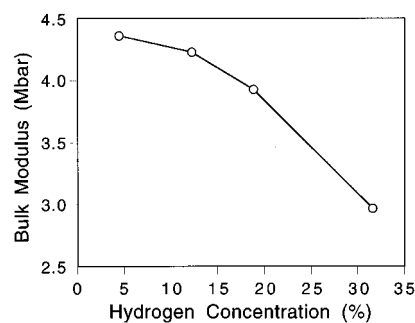


FIG. 5. Bulk modulus (in Mbars) as a function of the at. % hydrogen concentration.

simulation using classical potential.¹⁰ Recently, Weiler *et al.*⁶ have tried to relate the hardness of the ta-C:H films to the sp^3 fraction of the films. Our simulation results suggest that the hardness of ta-C:H films may not be directly proportional to the fraction of the sp^3 bonds, but rather to the fraction of sp^3 C-C bonds. For example, the samples with 50 and 100 hydrogen atoms exhibit almost the same sp^3 fraction but very different bulk modulus. It seems that the softening behavior can be attributed to the reduction of C-C bonds induced by hydrogen atoms, as discussed above.

In summary, we have studied the influence of hydrogen on the structure and properties of tetrahedral a-C samples by tight-binding molecular-dynamics simulations. We found that hydrogen in a-C tends to break the C-C bonds and makes the tetrahedral a-C samples softer. The reduction of the number of C-C bonds in the network also induces electronic states in the gap region that make the a-C sample less transparent.

Ames Laboratory is operated for the U.S. Department of Energy by Iowa State University under Contract No. W-7405-Eng-82. This work was supported by the Director for Energy Research, Office of Basic Energy Sciences, and the High Performance Computing and Communications Initiative, including a grant of computer time at the National Energy Research Supercomputing Center.

*Present address: Laboratoire Léon Brillouin (CEA-CNRS), Centre d'Etudes de Saclay, 91191 Gif-sur-Yvette CEDEX, France.

¹For a review, see J. Robertson, *Adv. Phys.* **35**, 317 (1986), and in *Diamond and Diamond-like Films and Coatings*, edited by R. Clausing *et al.*, NATO Advanced Study Institutes Ser. B, Physics, Vol. 266 (Plenum, New York, 1991), p. 331.

²D. R. McKenzie, D. Muller, and B. A. Pailthorpe, *Phys. Rev. Lett.* **67**, 773 (1991).

³P. H. Gaskell, A. Saeed, P. Chieux, and D. R. McKenzie, *Phys. Rev. Lett.* **67**, 1286 (1991).

⁴K. W. R. Gilkes, P. H. Gaskell, and J. Robertson, *Phys. Rev. B* **51**, 12 303 (1995).

⁵S. D. Berger, D. R. McKenzie, and P. J. Martin, *Philos. Mag. Lett.* **57**, 285 (1988).

⁶M. Weiler, S. Sattel, T. Giessen, K. Jung, H. Ehrhardt, V. S. Veerasamy, and J. Robertson, *Phys. Rev. B* **53**, 1594 (1996), and references therein.

⁷Th. Frauenheim, P. Blaudeck, U. Stephan, and G. Jungnickel, *Phys. Rev. B* **48**, 4823 (1993).

⁸D. A. Dradold, P. A. Fedders, and M. P. Grumbach, *Phys. Rev. B* **54**, 9703 (1996).

⁹N. A. Marks, D. R. McKenzie, B. A. Pailthorpe, M. Bernasconi, and M. Parrinello, *Phys. Rev. Lett.* **76**, 768 (1996).

¹⁰J. Tersoff, *Phys. Rev. B* **44**, 12 039 (1991).

¹¹S. Iarlori, G. Galli, and O. Martini, *Phys. Rev. B* **49**, 7060 (1994).

¹²P. D. Godwin, A. P. Horsfield, A. M. Stoneham, S. J. Bull, I. J. Ford, A.

H. Harker, D. G. Pettifer, and A. P. Sutton, *Phys. Rev. B* **54**, 15 785 (1996).

¹³C. Z. Wang and K. M. Ho, *Phys. Rev. Lett.* **71**, 1184 (1993).

¹⁴C. Z. Wang, K. M. Ho, and C. T. Chan, *Comput. Mater. Sci.* **2**, 93 (1994).

¹⁵C. H. Xu, C. Z. Wang, C. T. Chan, and K. M. Ho, *J. Phys.: Condens. Matter* **4**, 6047 (1992).

¹⁶G. Kopidakis, C. Z. Wang, C. M. Soukoulis, and K. M. Ho, in *Microcrystalline and Nanocrystalline Semiconductors*, edited by R. W. Collins, C. C. Tsai, M. Hirose, F. Koch, and L. Brus, MRS Symposia Proceedings No. 358 (Materials Research Society, Pittsburgh, 1995), p. 73.

¹⁷C. Mijoule, J.-M. Leclercq, S. Odier, and S. Fliszar, *Can. J. Chem.* **63**, 1741 (1985).

¹⁸B. J. Min, Y. H. Lee, C. Z. Wang, K. M. Ho, and C. T. Chan, *Phys. Rev. B* **45**, 6839 (1992).

¹⁹E. Hirota, *J. Mol. Spectrosc.* **77**, 213 (1979).

²⁰Axel D. Becke, *J. Chem. Phys.* **96**, 2155 (1992), and experimental references therein.

²¹D. L. Gray and A. G. Robiette, *Mol. Phys.* **37**, 1901 (1979).

²²G. Kopidakis, Ph.D. thesis, Iowa State University, 1995.

²³P. Briddon, R. Jones, and G. M. S. Lister, *J. Phys. C* **21**, L1027 (1988).

²⁴C. H. Chou and S. K. Estreicher, *Phys. Rev. B* **42**, 9486 (1990).

²⁵G. Kern, J. Hafner, and G. Kresse, *Surf. Sci.* **366**, 445 (1996).

²⁶D. A. Papaconstantopoulos and E. N. Economou, *Phys. Rev. B* **24**, 7233 (1981).

²⁷J. H. Rose, John Ferrante, and John R. Smith, *Phys. Rev. Lett.* **47**, 675 (1981).